The RING Finger Ubiquitin E3 Ligase OsHTAS Enhances Heat Tolerance by Promoting H_2O_2-Induced Stomatal Closure in Rice[1]

Jianping Liu[2], Cuicui Zhang[2]*, Chuchu Wei, Xin Liu, Mugui Wang, Feifei Yu, Qi Xie, and Jumin Tu*

Institute of Crop Science, Zhejiang University, Hangzhou 310058, China (J.L., C.Z., C.W., X.L., M.W., J.T.); and State Key Laboratory of Plant Genomics, National Center for Plant Gene Research, Institute of Genetics and Developmental Biology, Chinese Academy of Sciences, Chaoyang District, Beijing 100101, China (F.Y., Q.X.)

Heat stress often results in the generation of reactive oxygen species, such as hydrogen peroxide, which plays a vital role as a secondary messenger in the process of abscisic acid (ABA)-mediated stomatal closure. Here, we characterized the rice (*Oryza sativa*) *HEAT TOLERANCE AT SEEDLING STAGE* (*OsHTAS*) gene, which plays a positive role in heat tolerance at the seedling stage. *OsHTAS* encodes a ubiquitin ligase localized to the nucleus and cytoplasm. *OsHTAS* expression was detected in all tissues surveyed and peaked in leaf blade, in which the expression was concentrated in mesophyll cells. *OsHTAS* was responsive to multiple stresses and was strongly induced by exogenous ABA. In yeast two-hybrid assays, OsHTAS interacted with components of the ubiquitin/26S proteasome system and an isoform of rice ascorbate peroxidase. *OsHTAS* modulated hydrogen peroxide accumulation in shoots, altered the stomatal aperture status of rice leaves, and promoted ABA biosynthesis. The results suggested that the RING finger ubiquitin E3 ligase OsHTAS functions in leaf blade to enhance heat tolerance through modulation of hydrogen peroxide-induced stomatal closure and is involved in both ABA-dependent and DROUGHT AND SALT TOLERANCE-mediated pathways.

Heat stress affects plant growth, seed germination, photosynthesis, respiration, water relation, and membrane stability in plants (Wahid et al., 2007) and is often accompanied by the generation of reactive oxygen species (ROS), such as hydrogen peroxide (H_2O_2), hydroxyl radical, superoxide anion radicals, and singlet oxygen (Liu and Huang, 2000; Mittler, 2002; Apel and Hirt, 2004; Song et al., 2014). H_2O_2 is a very stable ROS with a long half-life (approximately 1 ms) and is also more diffusive than other ROS (Levine et al., 1994), so it can readily escape from the organelle in which it was produced to the cytosol. H_2O_2 plays a dual role in plants: at low concentrations, it acts as a signal molecule involved in acclimatory signaling, triggering tolerance to various biotic and abiotic stresses; and at high concentrations, it leads to programmed cell death (Quan et al., 2008). H_2O_2 also acts as a key regulator in a broad range of physiological processes, such as senescence (Peng et al., 2005), photorespiration and photosynthesis (Noctor and Foyer, 1998), stomatal movement (Bright et al., 2006), the cell cycle (Mittler et al., 2004), and growth and development (Foreman et al., 2003). H_2O_2 is beginning to be accepted as a secondary messenger for signals generated by ROS because of its relatively long life and high permeability across membranes (Quan et al., 2008). The major ROS-scavenging mechanisms include superoxide dismutase (SOD), ascorbate peroxidase (APX), and catalase (CAT; Bowler et al., 1992; Willekens et al., 1997; Noctor and Foyer, 1998). CAT does not need a reductant to scavenge H_2O_2, while APX needs ascorbate to act as a reductant. However, CAT has a lower affinity for H_2O_2 (millimolar range) than APX (micromolar range; Mittler, 2002). Hence, APX might function as a fine regulator of intracellular ROS steady-state levels, possibly for signaling purposes, whereas CAT might function as a bulk remover of excess ROS production under stress conditions (Willekens et al., 1997; Noctor and Foyer, 1998; Mittler, 2002; Cruz de Carvalho, 2008).

It has been well established that the abscisic acid (ABA) signaling pathway affects plant adaptation to stress by controlling the internal water status in plants (Cutler et al., 2010; Hauser and Horie, 2010; Raghavendra et al., 2010; Joshi-Saha et al., 2011; Fujii and Zhu, 2012). Significant ABA accumulation occurs in response to water-deficient stress; the increased ABA content triggers

[1] This work was supported by the Chinese National Natural Science Foundation (grant nos. 30871502 and 31371592).

[2] These authors contributed equally to the article.

* Address correspondence to zhangcuicui@zju.edu.cn and jtu@zju.edu.cn.

The author responsible for distribution of materials integral to the findings presented in this article in accordance with the policy described in the Instructions for Authors (www.plantphysiol.org) is: Jumin Tu (jtu@zju.edu.cn).

J.T. conceived the original research plans; J.T. and C.Z. supervised the experiments; J.L. and C.Z. together performed most of the experiments; C.W. performed the histochemical GUS assay; X.L. performed the field experiments; M.W. provided technical assistance in transient expression assays; F.Y. and Q.X. provided technical assistance in the E3 ubiquitin ligase activity assay; C.Z. designed the experiments and analyzed the data; C.Z. and J.L. conceived the project and wrote the article with contributions from all the authors; J.T. supervised the writing.

www.plantphysiol.org/cgi/doi/10.1104/pp.15.00879

stomatal closure, thus reducing water loss (Schroeder et al., 2001; Hirayama and Shinozaki, 2007). ABA is synthesized through the cleavage of a C40 carotenoid originating from the 2-*C*-methyl-D-erythritol-4-phosphate pathway, followed by the conversion of zeaxanthin to neoxanthin via violaxanthin. Subsequently, 9-cis-epoxycarotenoid dioxygenase (NCED) cleaves violaxanthin and neoxanthin to xanthoxin, which is then oxidized to abscisic aldehyde and converted to ABA (Nambara and Marion-Poll, 2005). The cleavage step catalyzed by NCED is generally thought to be the rate-limiting step of ABA biosynthesis (Iuchi et al., 2000; Xiong and Zhu, 2003), and this enzyme is involved in both drought (Iuchi et al., 2001; Qin and Zeevaart, 2002) and salt stress (Barrero et al., 2006) responses.

In the process of ABA-mediated stomatal closure, H_2O_2 plays a vital role as a secondary messenger by elevating calcium levels in guard cells through the activation of plasma membrane calcium channels (Pei et al., 2000; Wang and Song, 2008). The ABA-activated SnRK2 protein kinase OPEN STOMATA1 phosphorylates NADP (NADPH) oxidase (AtrbohF), which functions to produce ABA-induced ROS in guard cells (Kwak et al., 2003; Sirichandra et al., 2009). The double mutation of two NADPH oxidase genes (*AtrbohD* and *AtrbohF*) impairs the ABA-induced H_2O_2 production and stomatal closure (Kwak et al., 2003). Recently, an ABA-independent stomatal closure mechanism was reported in rice (*Oryza sativa*). DROUGHT AND SALT TOLERANCE (DST), a zinc finger transcription factor, negatively regulates H_2O_2-induced stomatal closure by directly regulating the expression of genes related to H_2O_2 scavenging (Huang et al., 2009). OsSRO1c suppresses *DST* to positively regulate H_2O_2-induced stomatal closure (You et al., 2013).

RING (for really interesting new gene) finger proteins harbor special zinc-binding domains defined by the consensus sequence Cys-X_2-Cys-$X_{(9-39)}$-Cys-$X_{(1-3)}$-His-$X_{(2-3)}$-Cys/His-X_2-Cys-$X_{(4-48)}$-Cys-X_2-Cys, where X can be any amino acid (Lovering et al., 1993). Depending on the fifth conserved amino acid, RING fingers are mainly classified as C3H2C3 (RING-H2) type or C3HC4 (RING-HC) type (Freemont, 2000; Jackson et al., 2000; Lim et al., 2010, 2013b). In addition to the two canonical RING types, additional types of modified RING domains, named RING-V, RING-D, RING-S/T, RING-G, and RING-C2, have been identified in Arabidopsis (*Arabidopsis thaliana*; Kosarev et al., 2002; Stone et al., 2005). Proteins harboring a RING domain are believed to play a role as ubiquitin ligases (E3) for the recognition and ubiquitylation of substrate proteins (Stone et al., 2005; Lim et al., 2013a). A number of RING E3s have been reported to play crucial roles in the posttranslational regulation of plant hormone signaling pathways, such as ABA and environmental stresses (Lim et al., 2013b). The overexpression of the Arabidopsis RING-H2 gene, *XERICO*, confers drought tolerance by increasing ABA biosynthesis through the up-regulation of a key ABA biosynthesis gene, *AtNCED3* (Ko et al., 2006). In Arabidopsis, OSMOTICALLY RESPONSIVE GENE1 (HOS1), which harbors a RING-like domain, negatively regulates cold signal transduction (Lee et al., 2001). Hot pepper (*Capsicum annuum*) RING MEMBRANE-ANCHOR 1 HOMOLOG1 functions as an E3 ligase, ubiquitinating the plasma membrane aquaporin PIP2;1 under water-deficient conditions (Lee et al., 2009). The C3HC4 RING finger E3 ligase OsDIS1, which is predominantly localized in the nucleus, plays a negative role in drought stress tolerance through the transcriptional regulation of diverse stress-related genes and possibly through the posttranslational regulation of OsNek6 in rice (Ning et al., 2011). The rice RING finger E3 ligase HEAT AND COLD INDUCED1 drives the nuclear export of multiple substrate proteins, and its heterogenous overexpression enhances acquired thermotolerance (Lim et al., 2013a). A novel membrane-bound RING-V (C4HC3) protein from *Brassica napus*, BnTR1, is likely to be involved in mediating Ca^{2+} dynamics by regulating the activity of calcium channels, which further alters the transcription of heat shock factors and heat shock proteins contributing to plant thermotolerance (Liu et al., 2014).

In our previous study, we identified a local *indica* rice cultivar, cv HT54, that is able to tolerate a high temperature of 48°C for approximately 79 h at the seedling stage, and we mapped this novel thermotolerant locus between the molecular markers InDel5 and RM7364. The physical distance of the two molecular markers is 420 kb and includes a gene (LOC_Os09g15430) possibly involved in heat stress response, which was named rice *HEAT TOLERANCE AT SEEDLING STAGE* (*OsHTAS*; Wei et al., 2013). In this study, the molecular function of *OsHTAS* in heat tolerance was reported. *OsHTAS* RNA interference (RNAi) transgenic plants showed obviously reduced heat resistance, and the gain-of-function mutant *oshtas* and *OsHTAS*-overexpressing (OE) transgenic plants displayed significantly improved heat tolerance at the seedling stage. The *OsHTAS* gene encodes a ubiquitin E3 ligase, which is localized to both the nucleus and the cytoplasm, and was induced strongly by exogenous ABA. The results demonstrated that the E3 ubiquitin ligase OsHTAS enhanced heat tolerance by promoting H_2O_2 accumulation-induced stomatal closing in rice.

RESULTS

OsHTAS Plays a Positive Role in Heat Tolerance at the Seedling Stage

To survey the potential function of *OsHTAS* in the heat stress responses of rice, *OsHTAS* RNAi rice plants were produced with a 312-bp open reading frame region of *OsHTAS* as the target interference region (Fig. 1A; Supplemental Fig. S1A). Two independent RNAi lines (Ri-3 and Ri-15), in which the *OsHTAS* expression level was approximately one-tenth of that in wild-type cv Nipponbare (Fig. 1B), were selected for heat tolerance testing (45°C for 48 h at the 3.5- to 4.5-leaf stage). Both Ri-3 and Ri-15 plants were more sensitive to heat

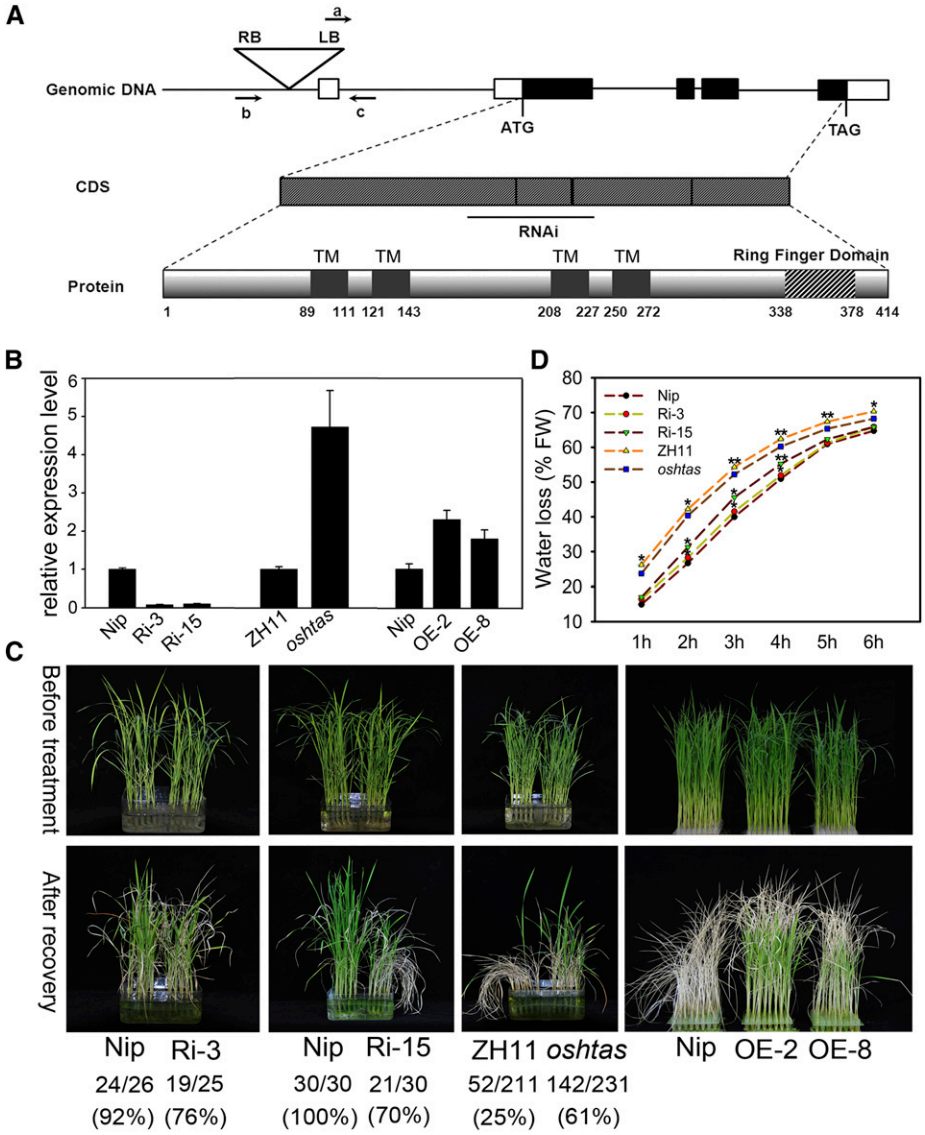

Figure 1. *OsHTAS* plays a positive role in heat tolerance at the seedling stage. A, Schematic diagram of the *OsHTAS* gene and the predicted OsHTAS protein. In the genomic DNA, exons, introns, and untranslated regions are indicated by black boxes, lines between boxes, and white boxes, respectively. The T-DNA insertion site is located in the promoter, 53 bp upstream of the transcription initiation site. LB, Left border of the T-DNA; RB, right border of the T-DNA. Arrows a, b, and c represent the primers used in the genotyping of the *oshtas* mutant. In the coding sequence (CDS), the black bar under the sequence indicates the target RNAi region (312 bp). In the protein sequence, four dark gray regions indicate the N-terminal transmembrane domains (TM), while the hatched bar shows the C-terminal RING finger domain. B, Expression analysis of *OsHTAS* in the RNAi lines (Ri-3 and Ri-15), the overexpressing lines (OE-2 and OE-8), and the *oshtas* mutant detected by quantitative real-time (qRT)-PCR. Nip, cv Nipponbare. Error bars indicate the SE based on three technical replicates. C, Heat tolerance tests of the wild type, the *oshtas* mutant, and several transgenic lines. Seedlings (3.5- to 4.5-leaf stage) grown in Yoshida solution were treated with a high-temperature (45°C) environment for the corresponding times (48 h for RNAi lines and 72 h for the *oshtas* mutant and overexpression lines), followed by culturing in normal conditions for 10 d. Survival rates were determined after 10 d of recovery. D, Water loss from detached leaves of cv Nipponbare, RNAi lines (Ri-3 and Ri-15), cv Zhonghua 11 (ZH11), and the *oshtas* mutant at the indicated time points. FW, Fresh weight. Error bars indicate the SE based on three technical replicates. *, $P < 0.05$ and **, $P < 0.01$, by Student's *t* test.

treatment than the wild type. The survival rates ranged from 76% to 70% for the *OsHTAS* RNAi lines and 92% to 100% for wild-type plants after 10 d of recovery (Fig. 1C). To verify the result, we prolonged the treatment time to 72 h, and all the survival rates decreased. The survival rates for Ri-3, Ri-15, and the wild type were 30%, 19%, and 57%, respectively (Supplemental Fig. S2). Furthermore, the water loss rates of detached leaves from Ri-3, Ri-15, and cv Nipponbare were measured. The results showed that the detached leaves of

both RNAi lines, especially Ri-15, lost water faster than the wild-type leaves (Fig. 1D). This increased water loss of the RNAi lines might lead to an increased sensitivity to high temperature.

To further confirm the *OsHTAS* function in heat tolerance, we searched the Rice Mutant Database (http://rmd.ncpgr.cn/) and found a transfer DNA (T-DNA) mutant (RMD_04Z11LZ47) corresponding to the *OsHTAS* gene (Wu et al., 2003; Zhang et al., 2006). Genotype analysis of the mutant indicated that the T-DNA tag was inserted into the promoter region, 53 bp upstream of the transcription initiation site (Fig. 1A; Supplemental Fig. S3). The *oshtas* mutant seedlings showed increased (approximately 5-fold) *OsHTAS* expression compared with wild-type cv ZH11; thus, this mutant was used as a gain-of-function mutant for further studies (Fig. 1B). Under normal growth conditions, the mutant *oshtas* appeared to have no obvious differences compared with the wild-type. Under heat stress (45°C for 72 or 96 h at the 3.5- to 4.5-leaf stage), the *oshtas* seedlings showed a strongly enhanced tolerance to heat stress, which was consistent with the behavior of the RNAi lines in heat treatment (Fig. 1C; Supplemental Fig. S2). The water loss rates of the detached leaves from *oshtas* were obviously lower than those of cv ZH11 (Fig. 1D), which was also consistent with the behavior of the RNAi lines.

In addition, we transformed the full-length coding sequence of *OsHTAS* under the control of the *ACTIN1* promoter into cv Nipponbare to produce the *OsHTAS*-OE lines (Supplemental Fig. S1B). Although *OsHTAS* expression in these overexpression lines was upregulated to approximately twice that of the wild-type plants, the OE-2 and OE-8 lines were more resistant to high temperature (45°C for 72 h at the 3.5- to 4.5-leaf stage) than the wild-type lines (Fig. 1, B and C). Taken together, all of these results suggested that *OsHTAS* plays a positive role in heat tolerance in rice.

OsHTAS Encodes a RING-H2 Finger Protein with Ubiquitin Ligase Activity in Vitro

The *OsHTAS* gene is composed of five exons and four introns (Fig. 1A), which was verified by the full-length complementary DNA (cDNA) sequence (Kikuchi et al., 2003; Satoh et al., 2007; Kawahara et al., 2013). The deduced protein consisting of 414 amino acids was predicted to be a zinc finger family protein by a BLASTP search of the Michigan State University database (http://rice.plantbiology.msu.edu/). InterProScan (http://www.ebi.ac.uk/Tools/InterProScan/) identified four transmembrane helices in the N terminus and a RING-H2-type finger domain at the C terminus of the OsHTAS protein, which implied that it has E3 ligase activity (Fig. 1A).

To test whether OsHTAS has ubiquitin ligase activity, we performed an in vitro ubiquitination assay. The attachment of ubiquitin (a small 76-amino acid protein) molecules to target substrates mediates a variety of cellular functions via the ubiquitin/26S proteasome system in higher plants (Lim et al., 2013b). In this pathway, the conjugation cascade requires three classes of enzymes: E1 (ubiquitin-activating enzyme), E2 (ubiquitin-conjugating enzyme), and E3 (ubiquitin ligase; Vierstra, 2009). The 142 amino acids of the C terminus of OsHTAS were expressed with a MALTOSE BINDING PROTEIN (MBP) tag and purified from *Escherichia coli*, and the self-ubiquitination activity of the protein was probed. The protein was incubated with wheat (*Triticum aestivum*) E1, human (*Homo sapiens*) E2 (UBCh5b), and ubiquitin, followed by immunoblot analysis. In the absence of E2 or MBP-RING, no polyubiquitination conjugates could be observed, whereas clear polyubiquitinated MBP-RING conjugates could be observed when all reagents were present (Fig. 2). These results were doubly confirmed by immunoblot analysis with anti-ubiquitin (Fig. 2A) and anti-MBP (tagged to RING; Fig. 2B; Supplemental Fig. S4) antibodies. These results also indicated that OsHTAS is a functional E3 ligase in vitro.

Subcellular Localization of OsHTAS

To study the subcellular localization of the OsHTAS protein, we fused the coding sequence of OsHTAS to yellow fluorescent protein (YFP) driven by the cauliflower mosaic virus 35S promoter (35S:YFP-OsHTAS) and delivered the construct into the epidermis of *Nicotiana benthamiana* by agroinfiltration (Supplemental Fig. S1C). The transgenic recipient was a nuclear marker *N. benthamiana* line expressing red fluorescent protein (RFP) fused with histone 2B (H2B; Martin et al., 2009). According to the YFP signal, the OsHTAS protein was localized to the nucleus and the cytoplasm (Fig. 3A).

We also assayed the localization using rice protoplasts. The full-length *OsHTAS* coding sequence was fused to the GFP-coding sequence under the control of the 35S promoter (35S:OsHTAS-GFP), which was transiently expressed with the endoplasmic reticulum marker RFP-HDEL (Nelson et al., 2007; De Caroli et al., 2011) in rice protoplasts (Supplemental Fig. S1D). The endoplasmic reticulum is contiguous with the nuclear envelope and surrounds the nucleus on all sides; the fluorescence indicated that the fusion protein was localized mainly to the nucleus and partially to the cytoplasm (Fig. 3B). At the same time, we used the rice nuclear protein RPL1 fused with cyan fluorescent protein (CFP) as a nuclear marker (Zhang et al., 2012) and cotransformed it into rice protoplasts with 35S:OsHTAS-GFP. The cyan fluorescence overlapped with the green fluorescence (Fig. 3B). Thus, both results showed that the OsHTAS protein has nuclear and cytoplasmic localization.

Expression Pattern of *OsHTAS*

Samples, including root and shoot, stem, blade and sheath of flag leaf, and panicle, were prepared from cv Nipponbare plants. The mRNA abundance of *OsHTAS* was detected using qRT-PCR. *OsHTAS* transcripts were detected in all tissues surveyed and peaked in the blade of the flag leaf (Fig. 4A).

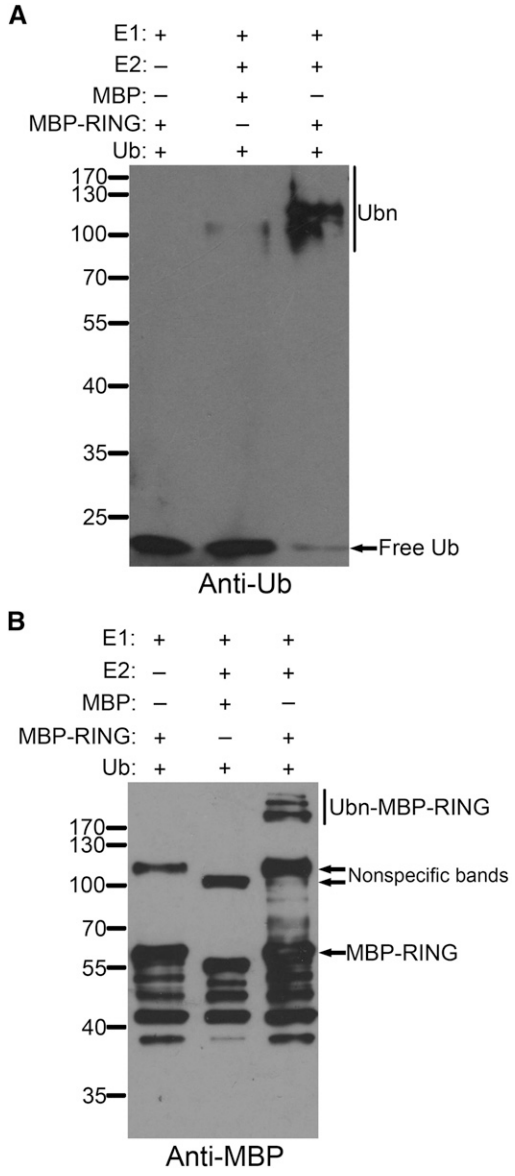

Figure 2. Ubiquitin ligase activity of OsHTAS in vitro. The MBP-RING (amino acids 273–414 of OsHTAS) fusion protein was assayed for ubiquitin ligase activity in the presence of wheat E1, human E2, and ubiquitin (Ub). The numbers on the left denote the molecular masses of marker proteins in kD. MBP was used as a negative control. Samples were resolved by 10% (w/v) SDS-PAGE. An antibody against ubiquitin was used to detect ubiquitin (A). An antibody against MBP was used to detect MBP fusion proteins (B). Ubn, Ubiquitin conjugates.

To further confirm the expression pattern of *OsHTAS*, we generated transgenic rice lines using the *GUS* reporter gene, which was under the control of the *OsHTAS* promoter (Supplemental Fig. S1E). DNA-blot hybridization analysis of five T_0 transgenic plants identified four plants harboring a single copy of the transgene, from which two transformants were chosen for histochemical staining to detect GUS activity (Supplemental Fig. S5). GUS expression was observed in the seedling root and shoot, leaf blade and sheath, and floret (Fig. 4B). In the seedling root, the GUS signal appeared in the vascular cylinders of both the adventitious and the lateral roots (Fig. 4B, images 1 and 2). In leaf blade and sheath, the GUS signal was concentrated in the mesophyll cells (Fig. 4B, images 3–6). In the floret, strong GUS expression was detected in the nerves and the margin of the lemma, the middle nerve of the palea, the vascular bundles of anthers, and the pistil, and weak GUS expression was detected in pollen grains (Fig. 4B, images 7–9).

To reveal the physiological and functional relevance of the *OsHTAS* gene, we further examined the expression level of *OsHTAS* under heat stress and other treatments, including cold, salt, polyethylene glycol (PEG), H_2O_2, and ABA, at the seedling stage. As shown in Figure 4C, after heat treatment, the *OsHTAS* transcripts decreased at 0.5 h and increased gradually to peak at 6 h, after which a gradual decrease occurred. In the cold and salt treatments, the situation was similar to the heat treatment, but the peaks for both treatments appeared at 12 h. After the PEG treatment, which mimicked drought stress, the transcript abundance of *OsHTAS* was nearly unchanged, with a slight increase at 24 h (1.8-fold). In the H_2O_2 treatment, the *OsHTAS* expression was reduced at most time points, except for an increase at 3 h. The abundance of *OsHTAS* transcripts changed very little until 12 h after ABA treatment but was dramatically induced to approximately 22-fold at 12 h and then decreased to 4-fold at 24 h. Taken together, *OsHTAS* was strongly induced by exogenous ABA but only slightly induced (2- to 4-fold) by heat, cold, salt, PEG, and H_2O_2 treatments (Fig. 4C). These results indicated that *OsHTAS* is responsive to multiple stresses.

OsHTAS-Interacting Proteins Detected by Yeast Two-Hybrid Assays

Different from the known DNA-binding zinc finger domains, the RING domain appears to function as a protein-protein interaction domain (Lovering et al., 1993; Borden, 2000). Because of this, we investigated the OsHTAS-interacting proteins in the yeast (*Saccharomyces cerevisiae*) system. Three baits represented the full-length OsHTAS (BK-OsHTASF; amino acids 1–414), the RING finger domain at the C terminus (BK-RING; amino acids 338–414), and the remaining N-terminal domain (BK-OsHTASN; amino acids 1–337), and these baits were constructed to screen a prey cDNA library prepared from cv Nipponbare callus. BK-OsHTASF screening resulted in no positive interactions with any proteins, while BK-OsHTASN screening obtained the rice OsAPX8 (LOC_Os02g34810; Fig. 5A).

BK-RING screening identified four positive interacting proteins: a ubiquitin extension protein (S27a; LOC_Os05g06770), a ribosomal protein (40SRPS; LOC_Os07g42450), and two ubiquitin-conjugating enzymes (E2; LOC_Os01g46926 and LOC_Os02g16040; Fig. 5, B and C). The RING finger domains of E3s contain two zinc ions and serve as the catalytic core (Lorick

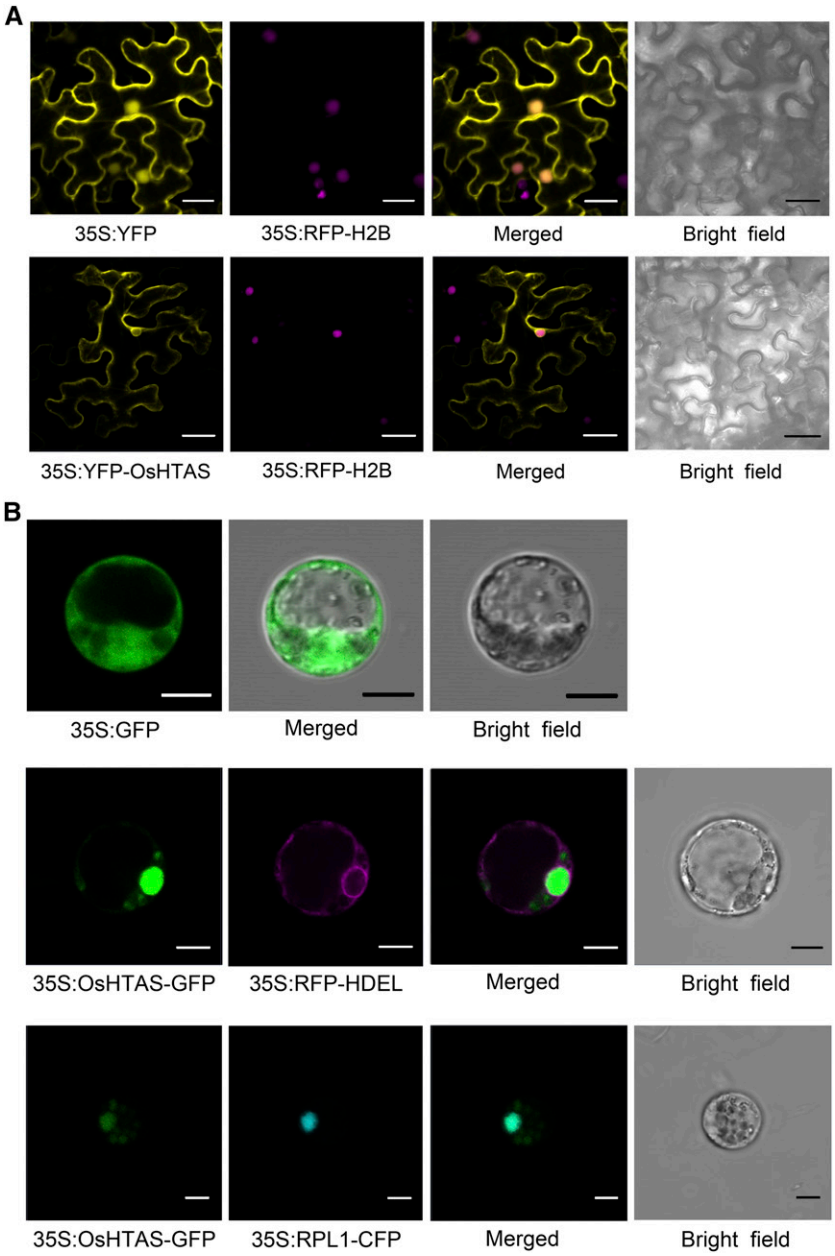

Figure 3. Subcellular localization of OsHTAS. A, Subcellular localization of OsHTAS in *N. benthamiana* epidermal cells. 35S:YFP-OsHTAS was delivered into the epidermis of *N. benthamiana* leaves expressing 35S:RFP-H2B (nuclear marker) by agroinfiltration. 35S:YFP was transformed using the same method as the control. Confocal images of the epidermal cells are shown. Bars = 20 μm. B, Subcellular localization of OsHTAS in rice protoplasts (cv ZH11 background). 35S:OsHTAS-GFP was cotransformed with 35S:RFP-HDEL (endoplasmic reticulum marker) or 35S:RPL1-CFP (nuclear marker) into rice etiolated shoot protoplasts. 35S:GFP was transformed as a control. Bars = 5 μm.

et al., 1999; Zheng et al., 2000). To test whether the intact RING finger domain (amino acids 338–378) of OsHTAS was indispensable to these interactions, two mutant constructs, BK-RING (H358Y) and AD-RING (H358Y), in which His-358 was changed to Tyr-358 (H358Y) to destroy the catalytic core, were used in the yeast two-hybrid assays (Supplemental Fig. S6). The interactions between RING and S27a and the two E2s disappeared, but the interaction between RING and 40SRPS was not affected, suggesting that RING interacted with S27a and the two E2s in the yeast two-hybrid assays and that the intact RING finger domain was critical for these interactions (Fig. 5, B and C).

We further investigated the expression levels of the interacting genes by qRT-PCR. All five OsHTAS-interacting genes were down-regulated in Ri-3, while they were up-regulated in *oshtas* plants (Fig. 5D). The above results indicated that the expression levels of these interacting genes were positively correlated with the expression level of *OsHTAS*.

OsHTAS Modulates ROS Homeostasis and Alters the Stomatal Aperture Status of Rice Seedlings

ROS are continuously produced as the by-products of various metabolic pathways and are scavenged by different antioxidative defense components in plants. The equilibrium between ROS production and scavenging may be perturbed by adverse environmental factors, such as heat stress (Apel and Hirt, 2004). As

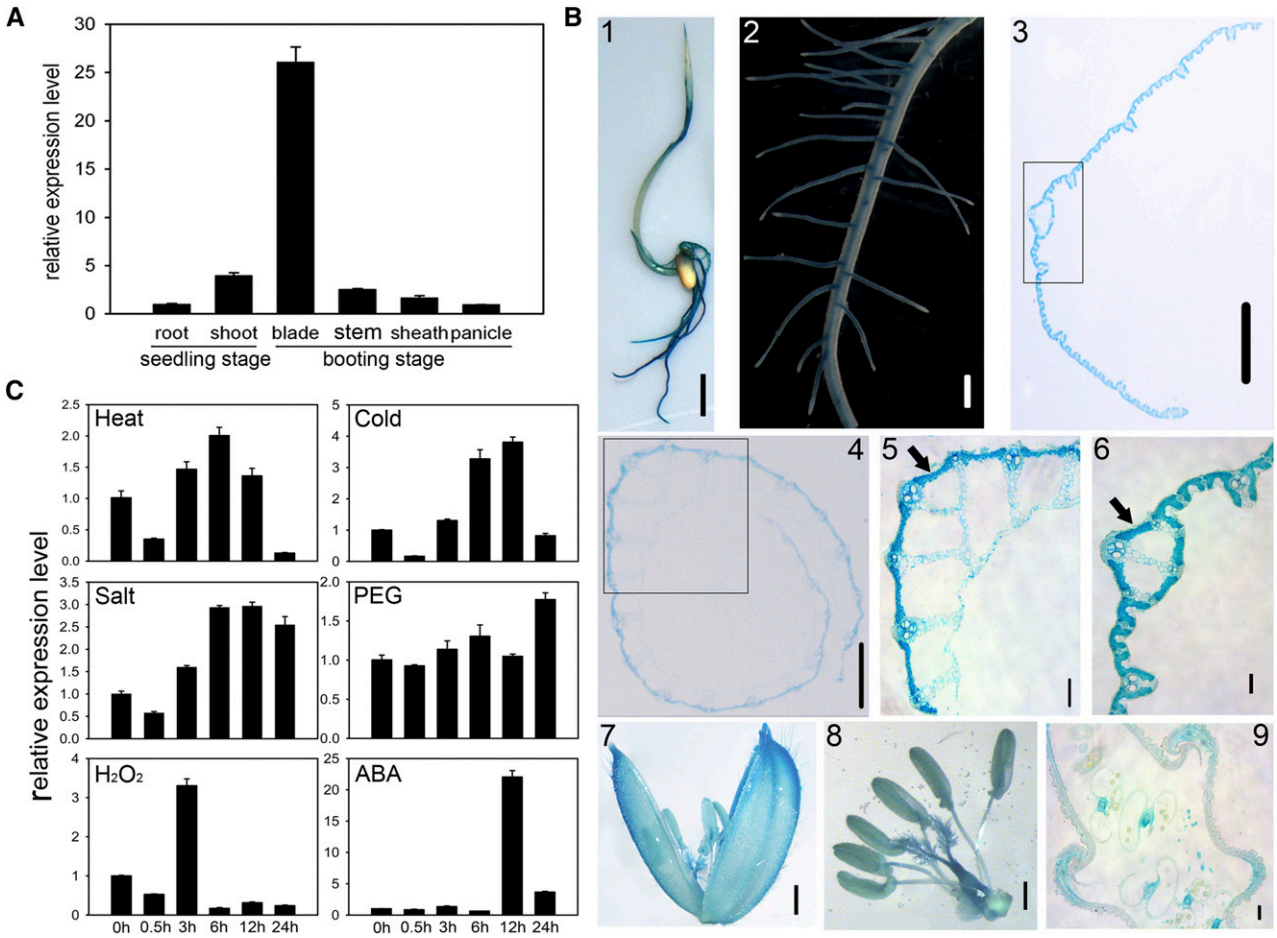

Figure 4. Expression pattern of *OsHTAS*. A, Expression analysis of *OsHTAS* in different tissues containing root, shoot, stem, blade and sheath of flag leaf, and panicle by qRT-PCR. Error bars indicate the SE based on three technical replicates. B, P_{OsHTAS}:*GUS* expression patterns in transgenic rice plants (cv Nipponbare background). GUS staining is shown in a 5-d-old seedling (1), root (2), and transverse sections of leaf blade, sheath, and floret (3, 4, and 9, respectively). 5 and 6 are magnified images of parts of 4 and 3, respectively. Black arrows indicate the mesophyll cells. 7 shows a floret, and 8 show pistils and stamens. Bars = 1 cm (1), 1 mm (2, 5, and 6–8), and 0.1 mm (3, 4, and 9). C, Expression of *OsHTAS* under abiotic stress conditions. Seedlings (3.5- to 4.5-leaf stage) were subjected to heat (45°C), cold (4°C), salt (250 mM NaCl), PEG (20% [w/v] PEG 4000), H_2O_2 (100 mM), and ABA (100 μM). Relative expression levels of *OsHTAS* were examined by qRT-PCR. Error bars indicate the SE based on three technical replicates.

H_2O_2 is a very stable ROS with a long half-life (Levine et al., 1994), we measured the H_2O_2 content in seedling shoots with or without heat treatment (45°C at the 3.5- to 4.5-leaf stage) to investigate the ROS balance. The *oshtas* mutant accumulated less H_2O_2 before treatment than did the wild type, and H_2O_2 contents increased greatly in *oshtas*, while they increased only slightly in the wild type after treatment (Fig. 6A). Thus, ROS homeostasis in *oshtas* seedlings was perturbed and more greatly disturbed by heat stress than in the wild type.

To survey whether the mutant phenotype resulted from enzymatic ROS-scavenging mechanisms, we tested the activities of APX and CAT, which detoxify H_2O_2 to water (Willekens et al., 1997). After a 24-h exposure to high temperatures, the APX activities increased, while the CAT activities decreased in both the *oshtas* mutant and wild-type plants (Fig. 6B). However, the *oshtas* mutant had lower APX and CAT activities than the wild type both before and after heat stress. Thus, the reduced activities of APX and CAT in *oshtas* might account for the higher H_2O_2 content of *oshtas* seedlings.

The H_2O_2 content and the APX and CAT activities were also measured in the *OsHTAS* RNAi lines (Ri-3 and Ri-15). Obvious decreases of H_2O_2 content were detected in both RNAi lines under both heat stress (45°C for 24 h at the 3.5- to 4.5-leaf stage) and normal conditions (Fig. 6C). Furthermore, we found that both RNAi lines had significantly higher APX and CAT activity levels than the wild-type plants under normal conditions (Fig. 6D).

The stomatal apertures of the *oshtas* mutant, the OsHTAS RNAi lines (Ri-3 and Ri-15), and the wild-type plants were investigated by scanning electron microscopy. No significant differences between the mutant and the wild type were detected before heat treatment

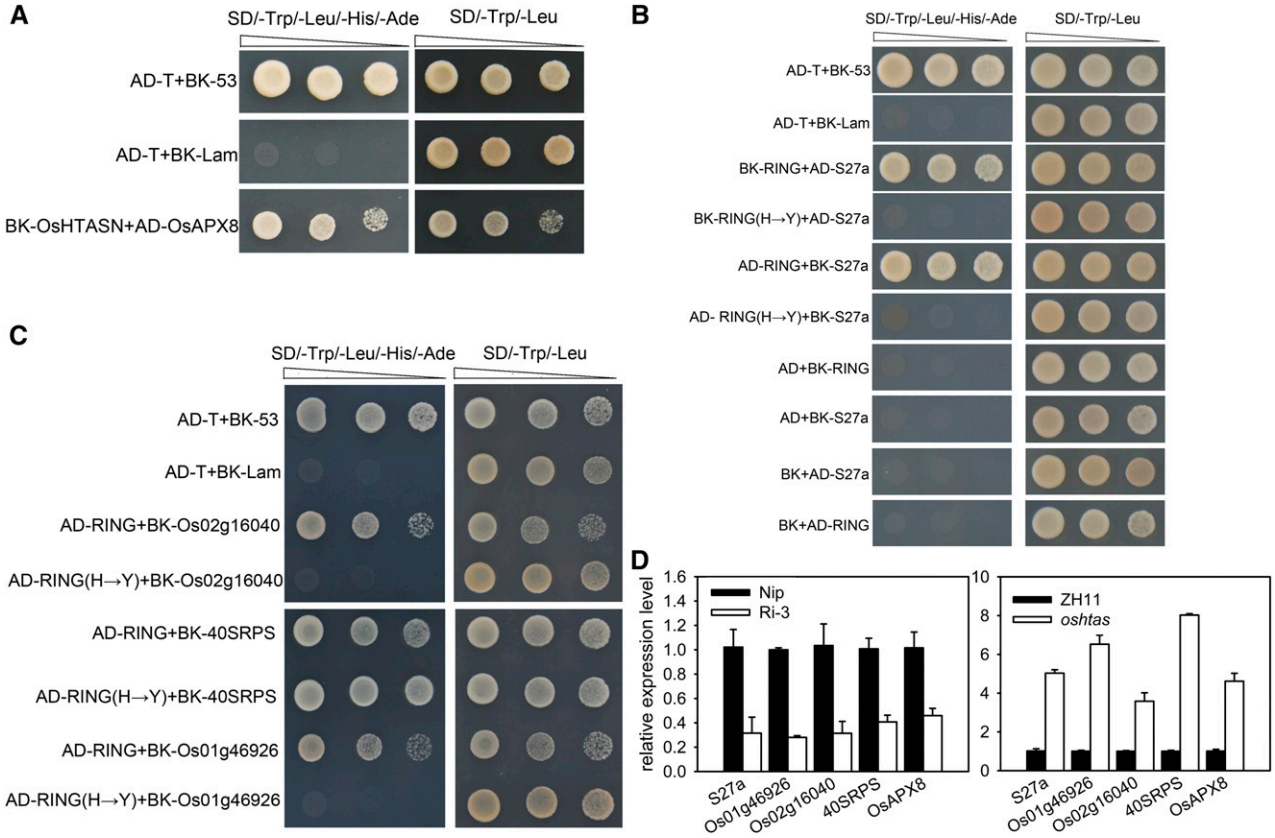

Figure 5. OsHTAS-interacting proteins identified by yeast two-hybrid analysis. A, Identification of the interaction between the N terminus of OsHTAS and OsAPX8. AD-T cells cotransformed with BK-53 or the BK-Lam vector were used as positive or negative controls. B, Identification of the interaction between the RING finger domain of OsHTAS and S27a. H→Y indicates that the 358th amino acid of OsHTAS was changed from His to Tyr. C, Identification of the interaction between the RING finger domain of the C terminus of OsHTAS and two ubiquitin-conjugating enzymes (E2; LOC_Os01g46926 and LOC_Os02g16040) and a ribosomal protein (40SRPS; LOC_Os07g42450). SD, Synthetic dextrose. D, Expression levels of all five OsHTAS-interacting genes in Ri-3 and *oshtas*. Error bars indicate the SE based on three technical replicates. Nip, cv Nipponbare.

(45°C for 24 h at the 3.5- to 4.5-leaf stage; Fig. 6, E and F). After the treatment, 53.8% of stomata were completely closed in the mutant plants, whereas 21% were completely closed in the wild-type plants. The rates of completely opened stomata were 11.5% and 48% in the *oshtas* and wild-type plants, respectively (Fig. 6F). Either before or after heat stress (45°C for 24 h at the 3.5- to 4.5-leaf stage), both RNAi lines had higher percentages of completely opened stomata than the wild type (before, 22.6% for Ri-3, 30.7% for Ri-15, and 18.1% for the wild type; after, 43.8% for Ri-3, 32.5% for Ri-15, and 21.3% for the wild type), while the percentages of completely closed stomata were lower in both compared with the wild-type (before, 31.2% for Ri-3, 19.3% for Ri-15, and 44.4% for the wild type; after, 12.5% for Ri-3, 11.7% for Ri-15, and 29.5% for the wild type; Fig. 6G). These results suggested that *OsHTAS* could promote stomatal closure.

OsHTAS Regulates ABA Biosynthesis

ABA regulates adaptive stress responses in plants (Cutler et al., 2010). *NCEDs* are known to be the key genes in controlling ABA biosynthesis; there are five *OsNCED* genes reported in rice (Saika et al., 2007; Zhu et al., 2009). The overexpression of *STRESS-RESPONSIVE NAC1* (*SNAC1*) enhanced the drought resistance of transgenic plants, partly due to ABA sensitivity to prevent water loss (Hu et al., 2006). OsbZIP23 is a major player in the bZIP family in rice and confers ABA-dependent drought and salinity tolerance (Xiang et al., 2008). To determine if the function of *OsHTAS* in heat stress is involved with ABA, the transcript levels of three well-characterized ABA-related genes, *OsNCED4* (Zhu et al., 2009), *SNAC1*, and *OsbZIP23*, were checked in *OsHTAS*-related materials and their wild-type plants. By comparing Ri-3, OE-2, and *oshtas* with their wild-type cv Nipponbare and cv ZH11 lines, we found that the transcript abundance levels for all three tested genes were positively correlated with the *OsHTAS* expression level (Fig. 7, A–C). Therefore, these results suggested that *OsHTAS* may be involved in ABA-dependent stress tolerance.

The abundance levels of *OsNCED4* transcripts were significantly increased in OE-2 (more than 60-fold) and *oshtas* (more than 550-fold; Fig. 7, B and C). Thus, we

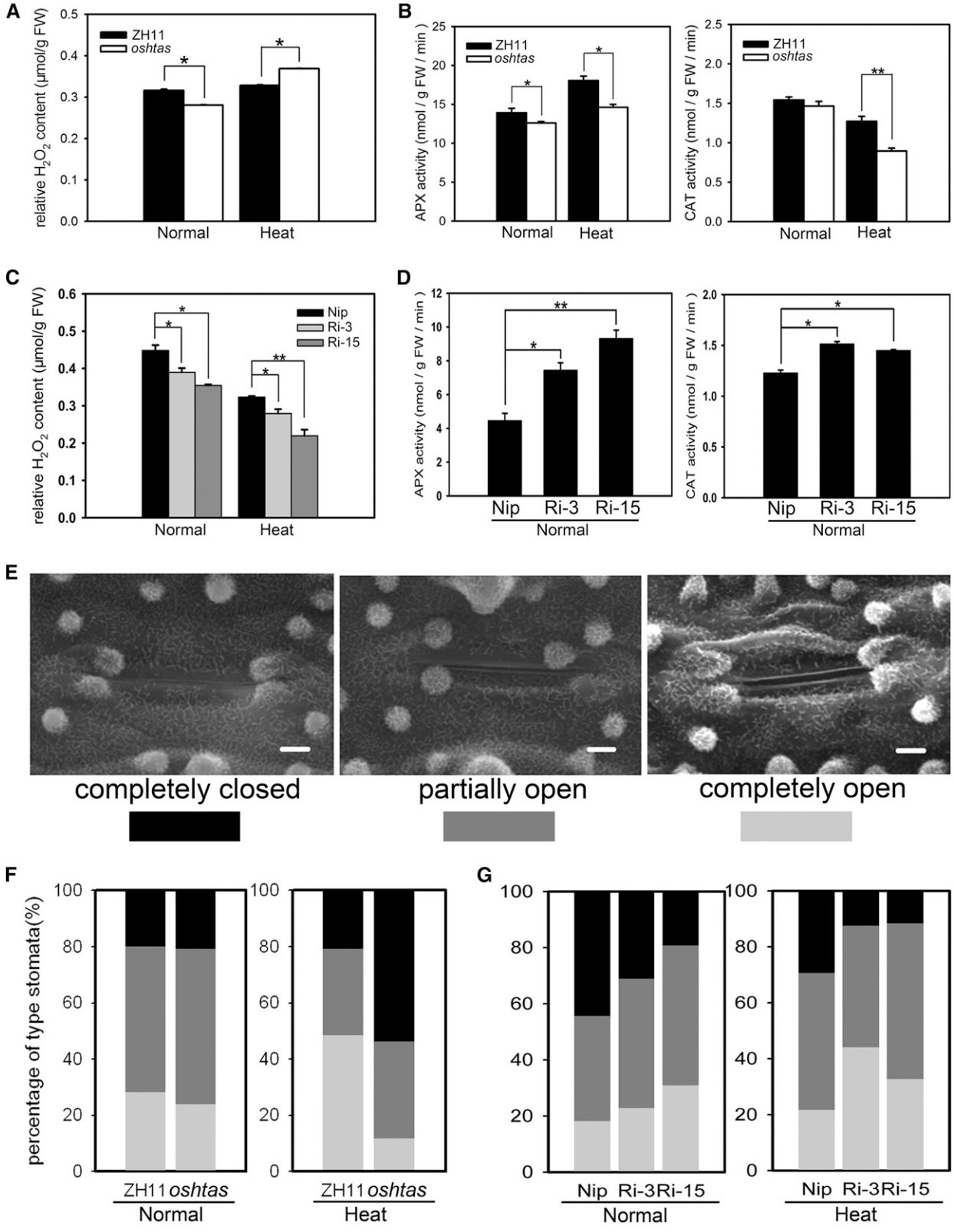

Figure 6. Modulated ROS homeostasis influenced the stomatal aperture status of rice leaves. A, Detection of the H_2O_2 content of cv ZH11 and *oshtas* mutant plants under normal and heat stress conditions. B, APX and CAT activities of cv ZH11 and *oshtas* mutant plants under normal and heat stress conditions. C, Detection of the H_2O_2 content of cv Nipponbare (Nip) and two RNAi lines (Ri-3 and Ri-15) under normal and heat stress conditions. D, APX and CAT activities of cv Nipponbare and two RNAi lines

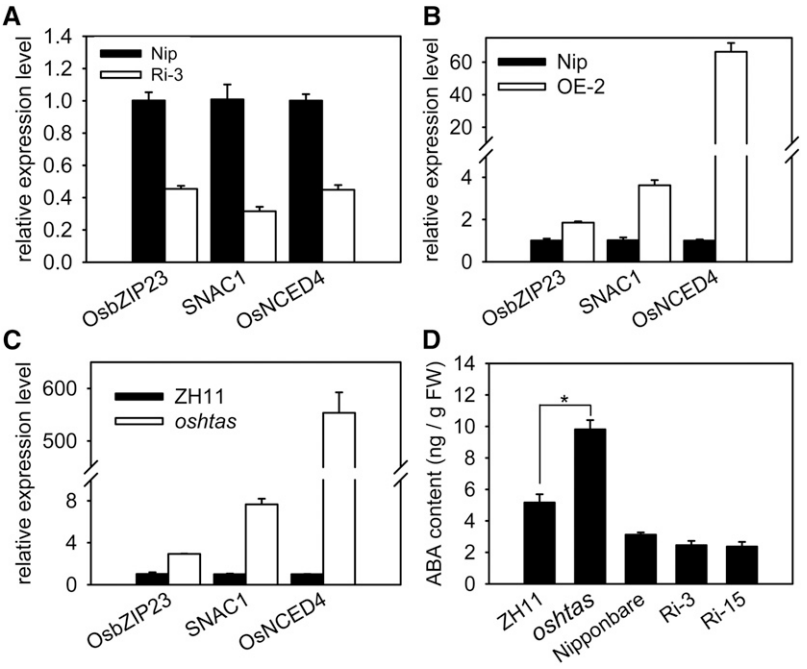

Figure 7. Expression levels of three ABA-related genes and ABA content measurements. A to C, Expression of three ABA-related genes (*SNAC1*, *OsbZIP23*, and *OsNCED4*) in the *OsHTAS* RNAi line (Ri-3), the overexpressing line (OE-2), and the gain-of-function mutant *oshtas*. Error bars indicate the SE based on three technical replicates. D, ABA contents of cv ZH11, the *oshtas* mutant, cv Nipponbare (Nip), Ri-3, and Ri-15 plants under normal conditions. FW, Fresh weight. Error bars indicate the SE based on three biological replicates. *, $P < 0.05$, by Student's *t* test.

measured the amounts of ABA in the shoots of the *oshtas* mutant and wild-type plants. The level of ABA in the *oshtas* mutant was approximately twice that in the wild-type plants (Fig. 7D). In Ri-3, *OsNCED4* expression was suppressed to half of that in cv Nipponbare. Therefore, we also measured the ABA contents in Ri-3 and Ri-15 and found that both RNAi lines had slightly reduced ABA contents compared with wild-type plants (Fig. 7D). These results indicated that *OsHTAS* plays a positive role in ABA biosynthesis.

DISCUSSION

The *OsHTAS* Gene Functions in Leaf Blade to Modulate H_2O_2 Content and Thus Enhances Basal Thermotolerance

Thermotolerance is the capacity of organisms to cope with excessively high temperatures and consists of basal and acquired thermotolerance (Song et al., 2012). Basal thermotolerance refers to the inherent capacity of an organism to survive exposure to temperatures above those optimal for growth, and acquired thermotolerance is induced by a short acclimation period at moderately high (but survivable) temperatures or by treatment with some other nonlethal stress prior to heat stress (Larkindale et al., 2005; Liu et al., 2015). In this study, *OsHTAS* was proven to promote the basal thermotolerance of rice seedlings (Fig. 1; Supplemental Fig. S2).

In yeast two-hybrid assays, the N terminus of OsHTAS interacted with OsAPX8 (Fig. 5A), which is putatively localized in the thylakoid (Teixeira et al., 2004). Additionally, OsHTAS was simultaneously localized to the nucleus and cytoplasm (Fig. 3). Taken together, it is possible that OsHTAS links chloroplasts with the nucleus, and the four transmembrane helices in the N terminus of OsHTAS may facilitate it passing through the membranes. The subcellular localization of plant RING E3 ligases can be changed by specific conditions (von Arnim and Deng, 1994). The Arabidopsis HOS1 protein resides in the cytoplasm at normal growth temperatures, but it accumulates in the nucleus in response to low temperature (Lee et al., 2001). Lim et al. (2014) found that 1 μM ABA treatment affects the translocation of OsCTR1 from chloroplasts to the cytosol. In our case, OsHTAS might alter its subcellular localization in response to heat stress. More research will be required to address this hypothesis. Chloroplasts are proposed to be heat sensors and are

Figure 6. (*Continued.*)
(Ri-3 and Ri-15) under normal conditions. FW, Fresh weight. Error bars indicate the SE based on three biological replicates. *, $P < 0.05$ and **, $P < 0.01$, by Student's *t* test. E, Scanning electron microscopy images of three levels of stomatal opening. Bars = 2 μm. F, Percentages of three levels of stomatal opening in cv ZH11 and *oshtas* mutant plants under normal and heat stress conditions (50 stomata for cv ZH11 under normal conditions; 40 stomata for *oshtas* under normal conditions; 29 stomata for cv ZH11 under heat conditions; and 26 stomata for *oshtas* under heat conditions). G, Percentages of three levels of stomatal opening in cv Nipponbare, Ri-3, and Ri-15 plants under normal and heat stress conditions (72 stomata for cv Nipponbare under normal conditions; 93 stomata for Ri-3 under normal conditions; 88 stomata for Ri-15 under normal conditions; 61 stomata for cv Nipponbare under heat stress conditions; 80 stomata for Ri-3 under heat stress conditions; and 120 stomata for Ri-15 under heat stress conditions).

massively distributed in mesophyll cells (Liu et al., 2015). *OsHTAS* expression peaked in the blade of flag leaf at the booting stage (Fig. 4A), and it was noted that the GUS signal of OsHTAS was especially concentrated in the mesophyll cells in leaf blade and sheath, while the signal localized on vascular bundles in all other organs (Fig. 4B).

H_2O_2 is an essential signaling molecule involved in the regulation of stomatal movement (Wang and Song, 2008; Yao et al., 2013). In the rice *dst* mutant, which confers drought, salt, and heat tolerance, H_2O_2 accumulation in guard cells led to stomatal closure (Huang et al., 2009; Shang, 2011). In this study, after heat treatment, the *oshtas* mutant closed more stomata, while RNAi lines opened more stomata compared with the wild type (Fig. 6, F and G). Additionally, the *oshtas* mutant had significantly lower H_2O_2 content before the heat treatment but had significantly higher H_2O_2 content after the treatment as compared with the wild-type plants (Fig. 6A). In addition, the *oshtas* mutant had lower APX activity than the wild type both before and after heat stress, and RNAi seedlings had higher APX activities than the wild type under normal conditions (Fig. 6, B and D). APX may function as a fine regulator of intracellular ROS steady-state levels for signaling purposes (Mittler, 2002; Cruz de Carvalho, 2008). Altogether, these data yield the hypothesis that *OsHTAS* may function in leaf blade, which is rich in mesophyll cells and stomatal pores, to modulate H_2O_2 content via APX during heat stress, thus enhancing the heat tolerance of rice.

OsHTAS Has E3 Ubiquitin Ligase Activity and Is Involved in Both ABA-Dependent and DST-Mediated Stomatal Closure

Ubiquitin extension proteins are composed of a single ubiquitin monomer fused to a carboxyl extension protein, which becomes associated with ribosomes (Callis and Vierstra, 1989; Finley et al., 1989; Chronis et al., 2013). The yeast two-hybrid assays revealed that the RING finger domain of OsHTAS interacted with a ribosomal protein, 40SRPS, a ubiquitin extension protein, S27a, and two E2s (Fig. 5, B and C). When the RING domain was changed via a point mutation, which disrupted the binding of zinc ions, the interactions of OsHTAS with S27a and two E2s disappeared (Fig. 5, B and C; Supplemental Fig. S6). In addition, we observed the subcellular localization of S27a in rice protoplasts through a CFP fusion with S27a (Supplemental Fig. S1F). These results demonstrated that CFP signal was in the nucleus overlapping with GFP representing OsHTAS (Supplemental Fig. S7). The subcellular distributions of the interacting proteins should be, at least partially, in common. These results also suggested that OsHTAS is an E3 ubiquitin ligase, which was already confirmed in the in vitro ubiquitination assay (Fig. 2). E3 ubiquitin ligases participate in plant responses to abiotic stress (Lee and Kim, 2011; Guo et al., 2013; Stone, 2014). The RING finger E3 ligase HOS1 mediates the ubiquitination and degradation of a MYC transcription factor (substrate of HOS1), which regulates the expression of cold-responsive genes to negatively regulate the cold response in Arabidopsis (Dong et al., 2006). The RING finger ubiquitin E3 ligase SDIR1 targets SDIR1-INTERACTING PROTEIN1 (substrate of SDIR1) for degradation, which selectively regulates the expression of the downstream basic region/Leu zipper motif transcription factor gene *ABA-INSENSITIVE5* to positively regulate ABA-mediated seed germination and the salt response in Arabidopsis (Zhang et al., 2015). Thus, it will be very helpful for the interpretation of the function of OsHTAS to find its substrate. By screening a callus prey library in the yeast two-hybrid assays, we found that OsAPX8 interacts with the N terminus of OsHTAS. Thus, it is necessary to test if OsHTAS can ubiquitinate OsAPX8, and if the interaction occurs in chloroplast in vivo, and thus regulate the H_2O_2 content. Furthermore, it makes sense to screen a prey library prepared from rice leaves treated with high temperatures.

A large number of ubiquitin ligases are involved with stress hormones; for example, at least 14 E3s have been linked to the regulation of ABA synthesis and signaling (Stone, 2014). The RING E3 ligase gene, *OsCTR1*, was strongly induced at 24 h under ABA treatment (Lim et al., 2014). In this study, *OsHTAS* expression was dramatically induced by exogenous ABA at 12 h (Fig. 4C), showing that *OsHTAS* responds to ABA slowly, which is similar to *OsCTR1*. The gain-of-function mutant *oshtas* dramatically increased *OsNCED4* expression and thus resulted in a higher level of ABA (Fig. 7, C and D), while Ri-3 had slightly lower ABA contents with decreased *OsNCED4* expression (Fig. 7, A and D). Previous studies indicated that ABA enhances cellular H_2O_2 production, which results in stomatal closure (Song et al., 2014). Accordingly, the reduced ABA was accountable for the lower H_2O_2 content and, hence, more open stomata in RNAi lines. Thus, *OsHTAS* regulates the ABA biosynthesis pathway and modulates H_2O_2-induced stomatal closure via the ABA signaling pathway.

The *DST* gene negatively regulates stomatal closure by inhibiting the accumulation of H_2O_2 content in rice leaves (Huang et al., 2009), and the loss-of-function mutant *dst* displayed more tolerance to heat stress (day/night, 42°C/37°C, 13 h/11 h; relative humidity, 30%; 3 d) than the wild-type cv ZH11 (Shang, 2011). *OsSRO1c*, a direct target gene of the transcription factor SNAC1, promoted stomatal closure through *DST* suppression and H_2O_2 accumulation in guard cells (You et al., 2013), and the mutant *ossro1c-1* with defective *OsSRO1c* showed greater sensitivity to heat stress (42°C for 48 h) compared with the wild type (J. You, personal communication). Closing stomata might be an effective method to prevent water loss from osmotic stress caused by high temperature. Nevertheless, our Ri-3 seedlings, in which the *SNAC1* expression level was approximately one-third of that in the wild type, had more opened and fewer closed stomata (Fig. 6F). This result is consistent

with a previous study in which there were significantly ($P < 0.01$) more stomatal pores that were closed in *SNAC1*-overexpressing transgenic rice than in the wild-type line under normal conditions (Hu et al., 2006). *DST* expression levels in the RNAi line Ri-3 and the gain-of-function mutant *oshtas* were also determined. *DST* expression was insignificantly increased in the Ri-3 line and obviously decreased in *oshtas* (Supplemental Fig. S8). Thus, *OsHTAS* may also be involved in DST-mediated H_2O_2-induced stomatal closure.

In conclusion, the ubiquitin E3 ligase OsHTAS functions in leaf blade to promote H_2O_2 production to induce stomatal closure during heat stress, thus enhancing rice heat tolerance. *OsHTAS* not only regulates the ABA-mediated H_2O_2-induced stomatal closure pathway but is also involved in DST-mediated stomatal closure, which is ABA independent and negatively regulates stomatal closure by inhibiting H_2O_2 production. This study increases our insights into the molecular mechanisms of rice responses to heat stress and may ultimately be helpful for the breeding of rice with heat adaptability.

MATERIALS AND METHODS

Plant Materials and Stress Treatments

RNAi transgenic plants were based on the rice (*Oryza sativa* ssp. *japonica*) 'Nipponbare' background. Overexpression and promoter-GUS fusion transgenic plants were based on the cv Nipponbare background. Mutant *oshtas* was in the cv ZH11 background.

To check the expression levels of the *OsHTAS* gene under various abiotic stresses or phytohormone treatment, cv Nipponbare rice plants were grown in Yoshida solution (Yoshida et al., 1976) for approximately 3 weeks under normal conditions. The seedlings at the 3.5- to 4.5-leaf stage were treated with abiotic stresses, including heat stress (exposing plants to 45°C), cold stress (seedlings were transferred to a growth chamber at 4°C), salt stress (treated with 250 mM NaCl), drought stress (treated with 20% [w/v] PEG 4000), oxidative stress (treated with 100 mM H_2O_2), and ABA treatment (100 μM ABA), followed by sampling at the designated times. We prepared each RNA sample with shoots from four seedlings and ensured that every sampled seedling was of the same growth stage.

For heat stress treatment, seeds were placed for 1 week or more at 42°C to break any possible dormancy, soaked in water for 3 or 5 d at 35°C, and then germinated for 1 d at 37°C. The uniformly germinated seeds were sown on 96-well plates whose bottoms were removed or in plastic boxes with blotting paper. Each plate or box was soaked in the Yoshida culture solution, which was then cultured in a growth chamber with a 13-h-light (25°C)/11-h-dark (25°C) photoperiod, 70% to 80% humidity, and 6,800 to 7,000 lx light intensity. Approximately d later, the seedlings were transferred into the freshly prepared Yoshida culture solution. The 3.5- to 4.5-leaf stage seedlings were transferred to a growth chamber with a 13-h-light (45°C)/11-h-dark (45°C) photoperiod, 70% to 80% humidity, and 23,800 lx light intensity for 2 to 4 d. The treated seedlings were placed back into the previous growth conditions for recovery, and seedlings with newly growing leaf blades were then counted as surviving plants.

Vector Construction and Plant Transformation

To construct the overexpression vector, the full-length coding sequence of *OsHTAS* was obtained from the cDNA of cv Nipponbare and inserted into the pMD18T vector (Takara). The resulting construct, called pMD18T-*OsHTAS*, was then confirmed by sequencing with M13F and M13R primers. The sequence-confirmed clone containing the coding sequence of *OsHTAS* was digested with *Pst*I and *Sma*I and subsequently subcloned into the modified pCAMBIA1300 vector (target gene driven by a rice *ACTIN1* promoter). To construct the RNAi vector, the PCR products that were amplified from pMD18T-*OsHTAS* using the primers OsHTAS RNAi-F and OsHTAS RNAi-R (Supplemental Table S1) were digested with two pairs of restriction enzymes: *Kpn*I/*Bam*HI and *Spe*I/*Sac*I, respectively. The differently digested fragments were then successively cloned into pTCK303 vector to produce the RNAi construct. To construct the P_{OsHTAS}:GUS vector, the PCR products that were amplified from cv Nipponbare genomic DNA using the primers GUS-F and GUS-R (Supplemental Table S1) were digested with the restriction enzymes *Hin*dIII and *Sal*I. The fragments were then cloned into DX2181 vector to produce the promoter-GUS fusion construct.

The resulting constructs were introduced into cv Nipponbare by *Agrobacterium tumefaciens*-mediated transformation. The transformants were then screened by PCR amplification using primers specific for the *HYGROMYCIN B PHOSPHOTRANSFERASE* gene (Supplemental Table S1).

Subcellular Localization of OsHTAS

Coding sequences of the target genes were amplified by PCR and directionally inserted into pCAMBIA1300-35S:YFP-NOS and/or the transient expression vector pM999-GFP or pM999-CFP. The cultures of the *A. tumefaciens* strain EHA105 harboring pCAMBIA1300-35S:YFP-NOS constructs were used to infect the healthy leaves of *Nicotiana benthamiana* (4 weeks old) expressing 35S:RFP-H2B (nuclear marker). The constructs of the pM999 series were transferred into rice protoplasts using the procedures described by Yoo et al. (2007). The fluorescence signals were observed using a confocal microscope (Leica TCS SP5 or Zeiss LSM710).

RNA Extraction and qRT-PCR Analysis

Fresh plant tissues were harvested and immediately ground into fine powder in liquid nitrogen. Total RNAs were extracted using TRIzol reagent (Invitrogen) according to the manufacturer's instructions. The DNase-treated RNA was reverse transcribed using SuperScript III reverse transcriptase (Invitrogen) according to the manufacturer's instructions. qRT-PCR was performed on an optical 96-well plate with a CFX96 Real-Time PCR Detection System (Bio-Rad) or a LightCycler 96 Real-Time PCR System (Roche) using SYBR Premix Ex Taq (Takara). The PCR thermal cycling protocol was as follows: 95°C for 10 s, followed by 40 cycles at 95°C for 5 s and 60°C for 30 s. Primers for *OsAPX8* were from Chao et al. (2010). Primers for *OsNCED4*, *OsbZIP23*, and *SNAC1* were from Luo et al. (2014). Primers for other target genes were designed using the Roche Web site (Roche Applied Science). The rice *ACTIN1* gene was used as the internal reference (Zhang et al., 2012), and data analyses with the $2^{-\Delta\Delta Ct}$ method were performed as described (Livak and Schmittgen, 2001).

Histochemical GUS Assay

A genomic DNA sequence corresponding to 3,667 bp upstream of ATG was amplified and then cloned into the DX2181 binary vector. The accuracy of the insert was verified by DNA sequencing. This construct was introduced into cv Nipponbare using *A. tumefaciens* strain EHA105. To detect GUS activity, 3-week-old transgenic plants were placed into GUS staining solution (1 mM 5-bromo-4-chloro-3-indolyl-β-D-GlcA, 0.1 M $Na_2H_2PO_4$, 10 mM Na_2EDTA, 0.5 mM potassium ferrocyanide, 0.5 mM potassium ferricyanide, and 0.1% [v/v] Triton X-100, pH 7) and vacuum infiltrated to remove trapped air for 20 to 30 min. The plantlets were then incubated at 37°C overnight. Chlorophyll was removed by washing with 70% (v/v) ethanol. Plants were visualized with a dissecting microscope (Leica MZ 95).

E3 Ubiquitin Ligase Activity Assay

The coding sequence (817–1,245 bp) containing the RING finger domain of *OsHTAS* was cloned into the pMAL-c2 vector (New England Biolabs), expressed in *Escherichia coli* Rosetta (DE3) as a fusion with MBP (MBP-RING), and purified according to the manufacturer's instructions. Crude extracts containing recombinant wheat (*Triticum aestivum*) E1 (GI: 136632), human (*Homo sapiens*) E2 (UBCh5b), MBP-RING, and ubiquitin (Beijing Thinkout Sci-Tech) were used for the ubiquitin ligase activity assay, as described by Zhao et al. (2013).

Yeast Two-Hybrid Assays

The coding sequences of the C terminus containing the RING finger domain (amino acids 338–414), the N terminus (amino acids 1–337), and the full-length OsHTAS protein were amplified and cloned in frame with the GAL4 DNA-binding domain of the pGBKT7 vector to generate GAL4 DNA-BD fusion constructs, called BK-RING, BK-OsHTASN, and BK-OsHTASF, respectively. The yeast (*Saccharomyces cerevisiae*) transformation and library screening were conducted in accordance with the recommended procedures (BD Matchmaker

Library Construction & Screening Kit). A rice cDNA library from the callus of cv Nipponbare was fused to the yeast GAL4 activation domain as prey protein and was collectively called the pGADT7-library. The BK-RING and pGADT7-library, or BK-OsHTASN and pGADT7-library, or BK-OsHTASF and pGADT7-library plasmids were cotransformed into AH109 yeast cells, and the cotransformed mixtures were spread on synthetic dextrose/–Ade/–His/–Leu/–Trp plates. These plates were then incubated at 30°C until colonies appeared. The library transformants may contain more than one AD-library plasmid, which may complicate the analysis of putative positive clones. Thus, we restreaked the positive colonies on synthetic dextrose/–Ade/–His/–Leu/–Trp plates two to three times to segregate the AD-library plasmids. To identify the gene responsible for a positive yeast two-hybrid interaction, we rescued the gene by PCR using the 5′-AD and 3′-AD screening primers. We sequenced the PCR products and BLAST searched the sequences in the National Center for Biotechnology Information database. To confirm the interactions, the coding sequences of the target genes were cloned into pGADT7 and/or pGBKT7 vectors to retest the interactions by the cotransformation of different plasmid combinations into AH109 yeast cells.

Measurement of H_2O_2 and ABA Contents and Detection of APX and CAT Activities

Shoots harvested from 3.5- to 4.5-leaf stage seedlings, with or without heat treatment, were used to measure H_2O_2 contents. The contents were measured spectrophotometrically after reaction with potassium iodide. The reaction mixture consisted of 0.5 mL of 0.1% (w/v) TCA, leaf extract supernatant, 0.5 mL of 100 mM potassium phosphate buffer (pH 7.8), and 1 mL of reagent (1 M [w/v] potassium iodide in fresh double distilled water). The blank control consisted of 1 mL of 0.1% (w/v) TCA and 1 mL of potassium iodide in the absence of leaf extract. After 1 h of reaction in darkness, the absorbance was measured at 390 nm. The amount of H_2O_2 was calculated using a standard curve prepared with known concentrations of H_2O_2. ABA contents were analyzed using gas chromatography-mass spectrometry as described (Fu et al., 2012). APX and CAT activities were determined according to Zeng et al. (2011).

Observation of Guard Cells and Detection of Water Loss Rate

Leaves of 3.5- to 4.5-leaf stage plants with or without heat treatment for 24 h were fixed with 2.5% (v/v) glutaraldehyde, and stomatal images (20 kV, 2,000×) were obtained using scanning electron microscopy (KYKY-EM3200).

To detect the water loss rate under dehydration conditions, shoots of positive transgenic plants and wild-type plants were cut, exposed to air temperature, and weighed at the designated times.

Accession numbers for the genes mentioned in this article are as follows: OsHTAS (AK069027.1, KU133655), SNAC1 (DQ394702), OsNCED4 (AK119780.1), OsbZIP23 (AK072062), and DST (GQ178286).

Supplemental Data

The following supplemental materials are available.

Supplemental Figure S1. Schematic of constructs in this study.

Supplemental Figure S2. Additional biological repeat for the heat tolerance test of the wild type, the *oshtas* mutant, and RNAi lines.

Supplemental Figure S3. Genotyping of the *oshtas* T-DNA insertion mutant.

Supplemental Figure S4. SDS-PAGE of MBP-RING and MBP proteins.

Supplemental Figure S5. Southern-blot analysis of P_{OsHTAS}:GUS transgenic plants.

Supplemental Figure S6. Schematic of OsHTAS C3H2C3 RING finger composition and the mutated amino acid in the RING finger.

Supplemental Figure S7. Colocalization of OsHTAS and S27a.

Supplemental Figure S8. Expression of *DST* in Ri-3 and the *oshtas* mutant.

Supplemental Table S1. Primers used in this study.

Received June 10, 2015; accepted November 11, 2015; published November 12, 2015.

LITERATURE CITED

Apel K, Hirt H (2004) Reactive oxygen species: metabolism, oxidative stress, and signal transduction. Annu Rev Plant Biol **55:** 373–399

Barrero JM, Rodríguez PL, Quesada V, Piqueras P, Ponce MR, Micol JL (2006) Both abscisic acid (ABA)-dependent and ABA-independent pathways govern the induction of NCED3, AAO3 and ABA1 in response to salt stress. Plant Cell Environ **29:** 2000–2008

Borden KL (2000) RING domains: master builders of molecular scaffolds? J Mol Biol **295:** 1103–1112

Bowler C, Van Montagu M, Inze D (1992) Superoxide dismutase and stress tolerance. Annu Rev Plant Biol **43:** 83–116

Bright J, Desikan R, Hancock JT, Weir IS, Neill SJ (2006) ABA-induced NO generation and stomatal closure in Arabidopsis are dependent on H_2O_2 synthesis. Plant J **45:** 113–122

Callis J, Vierstra RD (1989) Ubiquitin and ubiquitin genes in higher plants. Oxford Surv Plant Mol Cell Biol **6:** 1–30

Chao YY, Hong CY, Kao CH (2010) The decline in ascorbic acid content is associated with cadmium toxicity of rice seedlings. Plant Physiol Biochem **48:** 374–381

Chronis D, Chen S, Lu S, Hewezi T, Carpenter SCD, Loria R, Baum TJ, Wang X (2013) A ubiquitin carboxyl extension protein secreted from a plant-parasitic nematode Globodera rostochiensis is cleaved in planta to promote plant parasitism. Plant J **74:** 185–196

Cruz de Carvalho MH (2008) Drought stress and reactive oxygen species: production, scavenging and signaling. Plant Signal Behav **3:** 156–165

Cutler SR, Rodriguez PL, Finkelstein RR, Abrams SR (2010) Abscisic acid: emergence of a core signaling network. Annu Rev Plant Biol **61:** 651–679

De Caroli M, Lenucci MS, Di Sansebastiano GP, Dalessandro G, De Lorenzo G, Piro G (2011) Protein trafficking to the cell wall occurs through mechanisms distinguishable from default sorting in tobacco. Plant J **65:** 295–308

Dong CH, Agarwal M, Zhang Y, Xie Q, Zhu JK (2006) The negative regulator of plant cold responses, HOS1, is a RING E3 ligase that mediates the ubiquitination and degradation of ICE1. Proc Natl Acad Sci USA **103:** 8281–8286

Finley D, Bartel B, Varshavsky A (1989) The tails of ubiquitin precursors are ribosomal proteins whose fusion to ubiquitin facilitates ribosome biogenesis. Nature **338:** 394–401

Foreman J, Demidchik V, Bothwell JH, Mylona P, Miedema H, Torres MA, Linstead P, Costa S, Brownlee C, Jones JD, et al (2003) Reactive oxygen species produced by NADPH oxidase regulate plant cell growth. Nature **422:** 442–446

Freemont PS (2000) Ubiquitination: RING for destruction? Curr Biol **10:** R84–R87

Fu J, Chu J, Sun X, Wang J, Yan C (2012) Simple, rapid, and simultaneous assay of multiple carboxyl containing phytohormones in wounded tomatoes by UPLC-MS/MS using single SPE purification and isotope dilution. Anal Sci **28:** 1081–1087

Fujii H, Zhu JK (2012) Osmotic stress signaling via protein kinases. Cell Mol Life Sci **69:** 3165–3173

Guo L, Nezames CD, Sheng L, Deng X, Wei N (2013) Cullin-RING ubiquitin ligase family in plant abiotic stress pathways. J Integr Plant Biol **55:** 21–30

Hauser F, Horie T (2010) A conserved primary salt tolerance mechanism mediated by HKT transporters: a mechanism for sodium exclusion and maintenance of high K^+/Na^+ ratio in leaves during salinity stress. Plant Cell Environ **33:** 552–565

Hirayama T, Shinozaki K (2007) Perception and transduction of abscisic acid signals: keys to the function of the versatile plant hormone ABA. Trends Plant Sci **12:** 343–351

Hu H, Dai M, Yao J, Xiao B, Li X, Zhang Q, Xiong L (2006) Overexpressing a NAM, ATAF, and CUC (NAC) transcription factor enhances drought resistance and salt tolerance in rice. Proc Natl Acad Sci USA **103:** 12987–12992

Huang XY, Chao DY, Gao JP, Zhu MZ, Shi M, Lin HX (2009) A previously unknown zinc finger protein, DST, regulates drought and salt tolerance in rice via stomatal aperture control. Genes Dev **23:** 1805–1817

Iuchi S, Kobayashi M, Taji T, Naramoto M, Seki M, Kato T, Tabata S, Kakubari Y, Yamaguchi-Shinozaki K, Shinozaki K (2001) Regulation of drought tolerance by gene manipulation of 9-cis-epoxycarotenoid dioxygenase, a key enzyme in abscisic acid biosynthesis in *Arabidopsis*. Plant J **27:** 325–333

Iuchi S, Kobayashi M, Yamaguchi-Shinozaki K, Shinozaki K (2000) A stress-inducible gene for 9-cis-epoxycarotenoid dioxygenase involved in abscisic acid biosynthesis under water stress in drought-tolerant cowpea. Plant Physiol **123:** 553–562

Jackson PK, Eldridge AG, Freed E, Furstenthal L, Hsu JY, Kaiser BK, Reimann JD (2000) The lore of the RINGs: substrate recognition and catalysis by ubiquitin ligases. Trends Cell Biol **10:** 429–439

Joshi-Saha A, Valon C, Leung J (2011) A brand new START: abscisic acid perception and transduction in the guard cell. Sci Signal **4:** re4

Kawahara Y, de la Bastide M, Hamilton JP, Kanamori H, McCombie WR, Ouyang S, Schwartz DC, Tanaka T, Wu J, Zhou S, et al (2013) Improvement of the *Oryza sativa* Nipponbare reference genome using next generation sequence and optical map data. Rice (N Y) **6:** 4

Kikuchi S, Satoh K, Nagata T, Kawagashira N, Doi K, Kishimoto N, Yazaki J, Ishikawa M, Yamada H, Ooka H, et al (2003) Collection, mapping, and annotation of over 28,000 cDNA clones from *japonica* rice. Science **301:** 376–379

Ko JH, Yang SH, Han KH (2006) Upregulation of an Arabidopsis RING-H2 gene, *XERICO*, confers drought tolerance through increased abscisic acid biosynthesis. Plant J **47:** 343–355

Kosarev P, Mayer KF, Hardtke CS (2002) Evaluation and classification of RING-finger domains encoded by the Arabidopsis genome. Genome Biol **3:** RESEARCH0016

Kwak JM, Mori IC, Pei ZM, Leonhardt N, Torres MA, Dangl JL, Bloom RE, Bodde S, Jones JDG, Schroeder JI (2003) NADPH oxidase *AtrbohD* and *AtrbohF* genes function in ROS-dependent ABA signaling in *Arabidopsis*. EMBO J **22:** 2623–2633

Larkindale J, Hall JD, Knight MR, Vierling E (2005) Heat stress phenotypes of Arabidopsis mutants implicate multiple signaling pathways in the acquisition of thermotolerance. Plant Physiol **138:** 882–897

Lee H, Xiong L, Gong Z, Ishitani M, Stevenson B, Zhu JK (2001) The *Arabidopsis HOS1* gene negatively regulates cold signal transduction and encodes a RING finger protein that displays cold-regulated nucleocytoplasmic partitioning. Genes Dev **15:** 912–924

Lee HK, Cho SK, Son O, Xu Z, Hwang I, Kim WT (2009) Drought stress-induced Rma1H1, a RING membrane-anchor E3 ubiquitin ligase homolog, regulates aquaporin levels via ubiquitination in transgenic *Arabidopsis* plants. Plant Cell **21:** 622–641

Lee JH, Kim WT (2011) Regulation of abiotic stress signal transduction by E3 ubiquitin ligases in *Arabidopsis*. Mol Cells **31:** 201–208

Levine A, Tenhaken R, Dixon R, Lamb C (1994) H_2O_2 from the oxidative burst orchestrates the plant hypersensitive disease resistance response. Cell **79:** 583–593

Lim SD, Cho HY, Park YC, Ham DJ, Lee JK, Jang CS (2013a) The rice RING finger E3 ligase, OsHCI1, drives nuclear export of multiple substrate proteins and its heterogeneous overexpression enhances acquired thermotolerance. J Exp Bot **64:** 2899–2914

Lim SD, Hwang JG, Jung CG, Hwang SG, Moon JC, Jang CS (2013b) Comprehensive analysis of the rice RING E3 ligase family reveals their functional diversity in response to abiotic stress. DNA Res **20:** 299–314

Lim SD, Lee C, Jang CS (2014) The rice RING E3 ligase, OsCTR1, inhibits trafficking to the chloroplasts of OsCP12 and OsRP1, and its overexpression confers drought tolerance in *Arabidopsis*. Plant Cell Environ **37:** 1097–1113

Lim SD, Yim WC, Moon JC, Kim DS, Lee BM, Jang CS (2010) A gene family encoding RING finger proteins in rice: their expansion, expression diversity, and co-expressed genes. Plant Mol Biol **72:** 369–380

Liu J, Feng L, Li J, He Z (2015) Genetic and epigenetic control of plant heat responses. Front Plant Sci **6:** 267

Liu X, Huang B (2000) Heat stress injury in relation to membrane lipid peroxidation in creeping bentgrass. Crop Sci **40:** 503–510

Liu ZB, Wang JM, Yang FX, Yang L, Yue YF, Xiang JB, Gao M, Xiong FJ, Lv D, Wu XJ, et al (2014) A novel membrane-bound E3 ubiquitin ligase enhances the thermal resistance in plants. Plant Biotechnol J **12:** 93–104

Livak KJ, Schmittgen TD (2001) Analysis of relative gene expression data using real-time quantitative PCR and the $2^{(-\Delta\Delta C(T))}$ method. Methods **25:** 402–408

Lorick KL, Jensen JP, Fang S, Ong AM, Hatakeyama S, Weissman AM (1999) RING fingers mediate ubiquitin-conjugating enzyme (E2)-dependent ubiquitination. Proc Natl Acad Sci USA **96:** 11364–11369

Lovering R, Hanson IM, Borden KL, Martin S, O'Reilly NJ, Evan GI, Rahman D, Pappin DJ, Trowsdale J, Freemont PS (1993) Identification and preliminary characterization of a protein motif related to the zinc finger. Proc Natl Acad Sci USA **90:** 2112–2116

Luo C, Guo C, Wang W, Wang L, Chen L (2014) Overexpression of a new stress-repressive gene *OsDSR2* encoding a protein with a DUF966 domain increases salt and simulated drought stress sensitivities and reduces ABA sensitivity in rice. Plant Cell Rep **33:** 323–336

Martin K, Kopperud K, Chakrabarty R, Banerjee R, Brooks R, Goodin MM (2009) Transient expression in Nicotiana benthamiana fluorescent marker lines provides enhanced definition of protein localization, movement and interactions in planta. Plant J **59:** 150–162

Mittler R (2002) Oxidative stress, antioxidants and stress tolerance. Trends Plant Sci **7:** 405–410

Mittler R, Vanderauwera S, Gollery M, Van Breusegem F (2004) Reactive oxygen gene network of plants. Trends Plant Sci **9:** 490–498

Nambara E, Marion-Poll A (2005) Abscisic acid biosynthesis and catabolism. Annu Rev Plant Biol **56:** 165–185

Nelson BK, Cai X, Nebenführ A (2007) A multicolored set of *in vivo* organelle markers for co-localization studies in *Arabidopsis* and other plants. Plant J **51:** 1126–1136

Ning Y, Jantasuriyarat C, Zhao Q, Zhang H, Chen S, Liu J, Liu L, Tang S, Park CH, Wang X, et al (2011) The SINA E3 ligase OsDIS1 negatively regulates drought response in rice. Plant Physiol **157:** 242–255

Noctor G, Foyer CH (1998) Ascorbate and glutathione: keeping active oxygen under control. Annu Rev Plant Physiol Plant Mol Biol **49:** 249–279

Pei ZM, Murata Y, Benning G, Thomine S, Klüsener B, Allen GJ, Grill E, Schroeder JI (2000) Calcium channels activated by hydrogen peroxide mediate abscisic acid signalling in guard cells. Nature **406:** 731–734

Peng C, Ou Z, Liu N, Lin G (2005) Response to high temperature in flag leaves of super high-yielding rice Pei'ai 64S/E32 and Liangyoupeijiu. Rice Sci **12:** 179–186

Qin X, Zeevaart JA (2002) Overexpression of a 9-cis-epoxycarotenoid dioxygenase gene in *Nicotiana plumbaginifolia* increases abscisic acid and phaseic acid levels and enhances drought tolerance. Plant Physiol **128:** 544–551

Quan LJ, Zhang B, Shi WW, Li HY (2008) Hydrogen peroxide in plants: a versatile molecule of the reactive oxygen species network. J Integr Plant Biol **50:** 2–18

Raghavendra AS, Gonugunta VK, Christmann A, Grill E (2010) ABA perception and signalling. Trends Plant Sci **15:** 395–401

Saika H, Okamoto M, Miyoshi K, Kushiro T, Shinoda S, Jikumaru Y, Fujimoto M, Arikawa T, Takahashi H, Ando M, et al (2007) Ethylene promotes submergence-induced expression of *OsABA8ox1*, a gene that encodes ABA 8′-hydroxylase in rice. Plant Cell Physiol **48:** 287–298

Satoh K, Doi K, Nagata T, Kishimoto N, Suzuki K, Otomo Y, Kawai J, Nakamura M, Hirozane-Kishikawa T, Kanagawa S, et al (2007) Gene organization in rice revealed by full-length cDNA mapping and gene expression analysis through microarray. PLoS ONE **2:** e1235

Schroeder JI, Allen GJ, Hugouvieux V, Kwak JM, Waner D (2001) Guard cell signal transduction. Annu Rev Plant Physiol Plant Mol Biol **52:** 627–658

Shang YS (2011) Molecular and physiological studies on *hst*, a heat-shock tolerance mutant of rice (*Oryza sativa* L.). Master thesis. Zhejiang University, Hangzhou, China

Sirichandra C, Gu D, Hu HC, Davanture M, Lee S, Djaoui M, Valot B, Zivy M, Leung J, Merlot S, et al (2009) Phosphorylation of the Arabidopsis AtrbohF NADPH oxidase by OST1 protein kinase. FEBS Lett **583:** 2982–2986

Song L, Jiang Y, Zhao H, Hou M (2012) Acquired thermotolerance in plants. Plant Cell Tissue Organ Cult **111:** 265–276

Song Y, Miao Y, Song CP (2014) Behind the scenes: the roles of reactive oxygen species in guard cells. New Phytol **201:** 1121–1140

Stone SL (2014) The role of ubiquitin and the 26S proteasome in plant abiotic stress signaling. Front Plant Sci **5:** 135

Stone SL, Hauksdóttir H, Troy A, Herschleb J, Kraft E, Callis J (2005) Functional analysis of the RING-type ubiquitin ligase family of Arabidopsis. Plant Physiol **137:** 13–30

Teixeira FK, Menezes-Benavente L, Margis R, Margis-Pinheiro M (2004) Analysis of the molecular evolutionary history of the ascorbate peroxidase gene family: inferences from the rice genome. J Mol Evol **59:** 761–770

Vierstra RD (2009) The ubiquitin-26S proteasome system at the nexus of plant biology. Nat Rev Mol Cell Biol **10:** 385–397

von Arnim AG, Deng XW (1994) Light inactivation of Arabidopsis photomorphogenic repressor COP1 involves a cell-specific regulation of its nucleocytoplasmic partitioning. Cell **79:** 1035–1045

Wahid A, Gelani S, Ashraf M, Foolad MR (2007) Heat tolerance in plants: an overview. Environ Exp Bot **61:** 199–223

Wang P, Song CP (2008) Guard-cell signalling for hydrogen peroxide and abscisic acid. New Phytol **178:** 703–718

Wei H, Liu J, Wang Y, Huang N, Zhang X, Wang L, Zhang J, Tu J, Zhong X (2013) A dominant major locus in chromosome 9 of rice (*Oryza sativa* L.) confers tolerance to 48°C high temperature at seedling stage. J Hered **104:** 287–294

Willekens H, Chamnongpol S, Davey M, Schraudner M, Langebartels C, Van Montagu M, Inzé D, Van Camp W (1997) Catalase is a sink for H_2O_2 and is indispensable for stress defence in C3 plants. EMBO J **16:** 4806–4816

Wu C, Li X, Yuan W, Chen G, Kilian A, Li J, Xu C, Li X, Zhou DX, Wang S, et al (2003) Development of enhancer trap lines for functional analysis of the rice genome. Plant J **35:** 418–427

Xiang Y, Tang N, Du H, Ye H, Xiong L (2008) Characterization of OsbZIP23 as a key player of the basic leucine zipper transcription factor family for conferring abscisic acid sensitivity and salinity and drought tolerance in rice. Plant Physiol **148:** 1938–1952

Xiong L, Zhu JK (2003) Regulation of abscisic acid biosynthesis. Plant Physiol **133:** 29–36

Yao Y, Liu X, Li Z, Ma X, Rennenberg H, Wang X, Li H (2013) Drought-induced H_2O_2 accumulation in subsidiary cells is involved in regulatory signaling of stomatal closure in maize leaves. Planta **238:** 217–227

Yoo SD, Cho YH, Sheen J (2007) *Arabidopsis* mesophyll protoplasts: a versatile cell system for transient gene expression analysis. Nat Protoc **2:** 1565–1572

Yoshida S, Forno D, Cock J, Gomez K (1976) Routine procedure for growing rice plants in culture solution. *In* S Yoshida, ed, Laboratory Manual for Physiological Studies of Rice. International Rice Research Institute, Los Banos, Philippines, pp 61–66

You J, Zong W, Li X, Ning J, Hu H, Li X, Xiao J, Xiong L (2013) The SNAC1-targeted gene *OsSRO1c* modulates stomatal closure and oxidative stress tolerance by regulating hydrogen peroxide in rice. J Exp Bot **64:** 569–583

Zeng FR, Zhao FS, Qiu BY, Ouyang YN, Wu FB, Zhang GP (2011) Alleviation of chromium toxicity by silicon addition in rice plants. Agric Sci China **10:** 1188–1196

Zhang CC, Yuan WY, Zhang QF (2012) *RPL1*, a gene involved in epigenetic processes regulates phenotypic plasticity in rice. Mol Plant **5:** 482–493

Zhang H, Cui F, Wu Y, Lou L, Liu L, Tian M, Ning Y, Shu K, Tang S, Xie Q (2015) The RING finger ubiquitin E3 ligase SDIR1 targets SDIR1-INTERACTING PROTEIN1 for degradation to modulate the salt stress response and ABA signaling in *Arabidopsis*. Plant Cell **27:** 214–227

Zhang J, Li C, Wu C, Xiong L, Chen G, Zhang Q, Wang S (2006) RMD: a rice mutant database for functional analysis of the rice genome. Nucleic Acids Res **34:** D745–D748

Zhao Q, Tian M, Li Q, Cui F, Liu L, Yin B, Xie Q (2013) A plant-specific *in vitro* ubiquitination analysis system. Plant J **74:** 524–533

Zheng N, Wang P, Jeffrey PD, Pavletich NP (2000) Structure of a c-Cbl-UbcH7 complex: RING domain function in ubiquitin-protein ligases. Cell **102:** 533–539

Zhu G, Ye N, Zhang J (2009) Glucose-induced delay of seed germination in rice is mediated by the suppression of ABA catabolism rather than an enhancement of ABA biosynthesis. Plant Cell Physiol **50:** 644–651